Available online at www.sciencedirect.com
SCIENCE DIRECT
Computers and Chemical Engineering 30 (2005) 83–98
Computers & Chemical Engineering
www.elsevier.com/locate/compchemeng

Simulation of separation processes using finite volume method

P. Cruz, J.C. Santos, F.D. Magalhães, A. Mendes *

LEPAE-Departamento de Engenharia Química, Faculdade de Engenharia, Universidade do Porto, Rua Dr. Roberto Frias, 4200-465 Porto, Portugal

Received 17 February 2005; received in revised form 20 July 2005; accepted 2 August 2005
Available online 5 October 2005

Abstract

In this work we present a comparison of different discretization techniques, in the context of finite volume formulation, for the solution of separation processes involving adsorption, absorption and permeation.

The mathematical model developed assumes axially dispersed plug-flow, uniform bed/sorbent/membrane properties along the axial coordinate and negligible radial gradients. The algorithm used enforces both local and global flux conservation in space and time. The discretization of convection terms is made using unbounded schemes and bounded high-resolution schemes.

We use the same strategy for simulating three different separation processes: membrane permeation, pressure swing adsorption and simulated moving bed. In the case of membrane permeation we present simulation results of air separation using a polysulfone membrane and compare to ones of Coker et al. [Coker, D. T., Freeman, B. D., & Fleming, G. K. (1998). Modeling multicomponent gas separation using hollow-fiber membrane contactors. *AIChE Journal*, *44*, 1289]. In the case of pressure swing adsorption we study a small pressure swing adsorption unit for air separation as described by Santos et al. [Santos, J. C., Portugal, A. F., Magalhaes, F. D., & Mendes, A. (2004). Simulation and optimization of small oxygen pressure swing adsorption units. *Industrial and Engineering Chemistry Research*, *43*, 8328]. In the case of simulated moving bed we consider the glucose/fructose separation as described by Leão and Rodrigues [Leão, C. P., & Rodrigues, A. E. (2004). Transient and steady-state models for simulated moving bed processes: Numerical solutions. *Computers and Chemical Engineering*, *28*, 1725].

Our simulated results are particularly interesting for the case of transient highly convective separation problems, where standard procedures may lead to the appearance of unphysical oscillations in the computed solution due to the existence of sharp moving fronts.

Keywords: Gas separation; Adsorption; Absorption; Modeling; Dynamic simulation

1. Introduction

The simulation and optimization of adsorption, absorption and permeation separation processes have been under close study in the last decade (Cruz, Santos, Magalhães, & Mendes, 2003; Nilchan & Pantelides, 1998; Purnomo & Alpay, 2000; Zhang, Hidajat, Ray, & Morbidelli, 2002), due to the development of new (ad) (ab) sorbents with high sorption capacity and selectivity (Sherman, 1999) and membranes (polymeric and carbon molecular sieve based) with high permeabities and selectivities (Mendes, Magalhães, & Costa, 2003).

Transient sorption separation processes can be modeled by using convection-dominated partial differential equations (PDEs) for mass conservation in the fluid phase, ordinary differential equations (ODEs) for the sorption rate in the stationary phase, and eventually, algebraic equations for the sorption equilibrium between phases. The coupled system of partial differential equations should be solved numerically, because the analytic solution can only be derived for ideal conditions (normally under the following assumptions: isothermal system, instantaneous equilibrium between the fluid and the stationary phases, negligible pressure drop, linear isotherm and frozen concentration profile during pressure variation stages).

For solving such system of equations, two different numerical approaches are normally used. The first one consists on the simultaneous space and time discretization of each PDE, and then resolution of the resulting system of non-linear algebraic equations (for example: double collocation). The other approach consists on the spatial discretization of each PDE and subsequent integration of the resulting initial value problem of ordinary differential equations with an appropriate integrator (method of lines: MOL). Usually, the integrator used is

* Corresponding author. Tel.: +351 22 5081695; fax: +351 22 5081449.
E-mail address: mendes@fe.up.pt (A. Mendes).

0098-1354/$ – see front matter © 2005 Elsevier Ltd. All rights reserved.
doi:10.1016/j.compchemeng.2005.08.004

Nomenclature

A	area (m^2)
b_i	Langmuir affinity constant (Pa^{-1})
c	fluid phase molar concentration ($mol\,m^{-3}$)
C_v	valve parameter
d	diameter (m)
D_{ax}	effective axial dispersion coefficient ($m^2\,s^{-1}$)
D_M^e	effective homogeneous diffusion coefficient ($m\,s^{-1}$)
k	iteration or LDF coefficient, $k_i = 15D_{M,i}^e/r_p^2$ (1/s)
K_v	valve parameter
L	length column (module) (m) or permeability coefficient ($mol\,m^{-2}\,s^{-1}\,Pa^{-1}$)
n	number of stages
nc	number of mixture components
N	molar flow rate ($mol\,s^{-1}$)
p	pressure (Pa)
Pe	Peclet number, $Pe = u_{ref}L/D_{ax}$
Pur	product purity
q	molar concentration in the adsorbed phase ($mol\,kg^{-1}$)
q_{max}	isotherm parameter, maximum capacity ($mol\,kg^{-1}$)
r	radius (m)
$\Re$	universal gas constant ($J\,mol^{-1}\,K^{-1}$)
Rec	product recovery
t	time variable (s)
T	temperature (K)
u	average (interstitial molar) velocity ($m\,s^{-1}$)
x	dimensionless spatial coordinate, $x = z/L$
y	molar fraction
z	spatial coordinate (m)

Greek symbols

α_M	ratio between diffusivity coefficients, $\alpha_{i,M} = D_{i,M}^e/D_{ref} = k_i/k_{ref}$
β	pressure drop parameter
δ_F	membrane thickness (m)
ε_b	bed void fraction (ratio between the free volume and the total volume)
ε_p	particle porosity
θ	dimensionless time variable, $\theta = t/\tau_b$
μ	mixture viscosity ($kg\,m^{-1}\,s^{-1}$)
ρ_s	apparent particle density ($kg\,m^{-3}$)
τ_b	bed time constant, $\tau_b = L/u_{ref}$
ϕ	error of the solution
φ	ratio between bed time constant and particle diffusion time constant (LDF approximation), $\varphi = \tau_b k_{ref}$

Subscripts

i	component
in	feed stream (inlet)
out	outlet stream
pres	pressurization
prod	production
purg	purge
ref	reference
T	total

Superscripts

F	feed
H	high
L	low
P	permeate or purge
R	retentate
ST	storage tank
V	vent
0	standard temperature and pressure conditions (STP)
*	dimensionless variable

based on the backward differentiation formulas (BDF) (Byrne, Hindmarsh, Jackson, & Brown, 1977; Hindmarsh, 1974; Petzold, 1983), known as Gear method (Gear, 1971), which is suitable for the solution of stiff problems.

Different numerical methods are usually applied in space and time discretization: orthogonal collocation, orthogonal collocation on finite elements, Galerkin finite elements and finite differences. These numerical methods are normally unbounded, which means that unphysical oscillations can appear in the computed solution. In the context of finite volume formulation, Harten, Engquist, Osher, and Chakravarthy (1987) proposed the use of ENO (essentially non-oscillatory) schemes and Shu and Osher (Shu, 1997; Shu & Osher, 1988, 1989) the WENO (weighted ENO) schemes for the solution of partial differential equations in the presence of steep moving fronts.

The aim of this work is present a numerical algorithm for the solution of sorption and permeation problems that provide accurate, local and global flux conservation, and stable numerical results (without unphysical oscillations in the computed solution) even at shocks or discontinuities and to present a systematic comparison of different discretization techniques.

The remaining of the paper is organized as follows: first the mathematical model (mass balance equation, boundary conditions, momentum equation) is presented. Following is presented the implementation of the successive stages method and the finite volume method, as well as a small discussion on the implementation of non-linear high-resolution schemes and WENO schemes. The performance of different discretization techniques is presented for three different separation processes: membrane permeation, pressure swing adsorption and simulated moving bed. In the case of membrane permeation we simulate a permeation module for air separation using a polysulfone membrane as described by Coker, Freeman, and Fleming (1998). In the case of pressure swing adsorption we study a two column pressure swing adsorption unit for air separation as described by Santos, Portugal, Magalhaes, and Mendes (2004). In the case of simu-

lated moving bed we consider the glucose/fructose separation as described by Leão and Rodrigues (2004). The paper ends with a summary of the main conclusions.

2. Model equations

The proposed theoretical model considers a separation system with a sorbent (adsorbent or absorbent) or a membrane (Fig. 1). The following main assumptions are made: perfect gas behavior (where applicable), axially dispersed plug-flow, uniform bed/sorbent/membrane properties along the axial coordinate and negligible radial gradients. According to these assumptions, the model equations can be written as follows:

$$\text{Total mass balance :} \quad \frac{\partial c_T}{\partial t} = -\frac{\partial (u c_T)}{\partial z} - \sum_{i=1}^{nc} N_i = 0 \tag{1}$$

ith component mass balance :

$$\frac{\partial c_i}{\partial t} = \frac{\partial}{\partial z}\left(D_{ax}\, c_T \frac{\partial (c_i/c_T)}{\partial z} \right) - \frac{\partial (u c_i)}{\partial z} - N_i, \quad i = 1, \text{nc} \tag{2}$$

where c_T is the total molar concentration, u the average (interstitial) molar velocity, z the spatial coordinate, D_{ax} the effective axial dispersion coefficient, N_i the ith component molar flow rate, c_i the ith component molar concentration in fluid phase, t the time variable and nc the number of components in the mixture.

Eqs. (1) and (2) can be written in dimensionless form as follows:

$$\text{Total mass balance :} \quad \frac{\partial c_T^*}{\partial \theta} = -\frac{\partial (u^* c_T^*)}{\partial x} - \sum_{i=1}^{nc} N_i^* \tag{3}$$

ith component mass balance :

$$\frac{\partial c_i^*}{\partial \theta} = \frac{1}{Pe}\frac{\partial}{\partial x}\left[c_T^* \frac{\partial (c_i^*/c_T^*)}{\partial x} \right] - \frac{\partial (u^* c_i^*)}{\partial x} - N_i^* \tag{4}$$

where c_T^* is the dimensionless total molar concentration, $c_T^* = c_T/c_{ref}$; θ the dimensionless time variable, $\theta = t/\tau_b$, τ_b the bed time constant, $\tau_b = L/u_{ref}$; u^* the dimensionless molar average velocity, $u^* = u/u_{ref}$; x the dimensionless axial coordinate, $x = z/L$; N_i^* the ith component dimensionless molar flow rate, $N_i^* = N_i \tau_b / c_{ref}$ and Pe the Peclet number for mass transfer, $Pe = u_{ref} L/D_{ax}$.

Eqs. (3) and (4) have initial values: $c_T^*(t, x) = c_T^*(0, x)$ and $c_i^*(t, x) = c_i^*(0, x)$. The term appearing on the left-hand side of Eq. (4) is called the inertia term, while on the right-hand side one can identify a convective (advective), a diffusive and a source term. When Eq. (4) is dominated by advection ($1/Pe \to 0$), it is called a hyperbolic PDE.

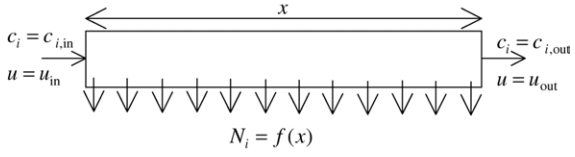

Fig. 1. Sketch of the model proposed for the solution of separation problems.

The application of conventional higher-order discretization schemes to the advective (convective) term, in the case of convection-dominated partial differential equation, may not be adequate leading to the appearance of non-physical oscillations (Finlayson, 1992). The upwind differencing scheme (UDS) proposed by Courant, Isaacson, and Rees (1952) is the only unconditionally stable scheme. This scheme, referred in the literature using different names: successive stages method, mixed cells in series model or cascade of perfectly mixed tanks, is well known in the context of separation processes (Charton & Nicoud, 1995; Cheng & Hill, 1985; Coker et al., 1998; Ludemann-Hombourger, Nicoud, & Bailly, 2000), however has only first-order accuracy, as will be seen in this work, and is not normally recommended (Freitas, 1994).

The implementation of ENO (essentially non-oscillatory) schemes (Harten et al., 1987) and WENO (weighted ENO) schemes (Shu, 1997; Shu & Osher, 1988, 1989) for the solution of partial differential equations, can reduce significantly the appearance of non-physical oscillations, however, these are normally very computation time consuming (Harten, 1996; Harten et al., 1987). Other approaches based on Harten's wavelet based framework (Harten, 1996) were proposed. The wavelet based ENO adaptative strategy may produce moderate CPU reductions, since in smooth regions the numerical fluxes are evaluated with inexpensive interpolations from surrounding grid points. However this reduction is rather limited, since for each time step the solution is still represented on the finest grid (Harten, 1996).

To overcome the occurrence of non-physical oscillations, when using higher-order discretization schemes, an extensive amount of research in computational fluid dynamics has been directed towards the development of accurate and bounded non-linear convective schemes. In this work we use high-resolution schemes (HRS), formulated in the context of the normalized variable and space formulation (NVSF) of Darwish and Moukalled (1994). These are, by definition, bounded higher-order schemes and will be briefly described below.

We perform the discretization of Eqs. (3) and (4) in two stages. Firstly, we compute the space derivatives appearing in the right-hand side using different schemes. Then, we integrate explicitly the resulting initial value problem in order to obtain the grid point values at the next time step. This time integration is performed with the package LSODA (Petzold, 1983), that is briefly described below.

For convenience, in the following sections the superscript "*" will be omitted from the dimensionless variables.

2.1. Boundary conditions

Eq. (4), the ith component mass balance equation, is a second-order differential equation and so it needs two boundary conditions. In separation processes, these boundary conditions are normally obtained from a balance in the vicinity of $x = 0$ and

$x = 1$.

$$x = 0: \quad \frac{1}{Pe}\frac{\partial(c_i/c_T)}{\partial x} = u_{x=0}\left(\frac{c_i - c_{i,x=0^-}}{c_T}\right) \tag{5}$$

$$x = 1: \quad \frac{1}{Pe}\frac{\partial(c_i/c_T)}{\partial x} = u_{x=1}\left(\frac{c_{i,x=1^+} - c_i}{c_T}\right) \tag{6}$$

These type of boundary conditions (Cauchy boundary conditions) are a weighted average of Dirichlet boundary conditions (which specify the value of the function) and Neumann boundary conditions (which specify the derivative of the function) and are known in the Chemical Engineering field as Danckwerts boundary conditions (Danckwerts, 1953).

When the velocity ($u_{x=0}$ or $u_{x=1}$) is equal to zero, Eqs. (5) and (6) are reduced to:

$$\frac{1}{Pe}\frac{\partial(c_i/c_T)}{\partial x} = 0 \tag{7}$$

Eq. (3), the total mass balance equation, is a first-order differential equation. Depending on the assumptions made, different boundary conditions can be applied. Following we present the most common, that should be useful for most of the problems.

2.1.1. Velocity profile in diluted systems

In diluted systems, for example purifications using pressure swing adsorption or simulated moving bed technologies, the total mass balance equation should not be solved, because the velocity profile can be considered constant:

$$u(\forall x) = u_{in} \tag{8}$$

where u_{in} is the molar average velocity in the feed stream.

2.1.2. Velocity profile without pressure drop (isothermal)

When the pressure drop and temperature variations can be considered negligible, two of the following three boundary conditions must be imposed:

$$u(x = 0) = u_{in} \tag{9}$$

$$u(x = 1) = u_{out} \tag{10}$$

$$\frac{\partial c_T}{\partial \theta} = \text{constant} \tag{11}$$

where u_{out} is the molar average velocity in the outlet stream.

2.1.3. Velocity profile with pressure drop (non-isothermal)

When the pressure drop and temperature variations cannot be considered negligible, one must impose one boundary condition in $x = 0$ and other in $x = 1$, as it follows:

$$u(x = 0) = u_{in} \quad \text{or} \quad c_T(x = 0) = c_{T,in} \tag{12}$$

$$u(x = 1) = u_{out} \quad \text{or} \quad c_T(x = 1) = c_{T,out} \tag{13}$$

2.2. Pressure drop

The pressure drop along a packed column or a hollow fiber permeation module can be described by the following equation (Bird, Stewart, & Lightfoot, 1960):

$$-\frac{\partial p_T}{\partial x} = \beta u \tag{14}$$

In the case of a permeation module, $\beta = 8\mu/r^2$, where μ is the mixture viscosity, given by Wilke's formula (Bird et al., 1960), and r the tube (or equivalent tube) radius. Eq. (14) results in the well-known Hagen–Poiseuille equation. In the case of packed columns, β should be:

$$\beta = \frac{150(1 - \varepsilon_b)^2}{\varepsilon_b^3 d_p^2} \tag{15}$$

where d_p is the particle diameter and ε_b the bed void fraction (bed porosity). Eq. (14) results in the also well-known Blake–Kozeny equation.

3. Successive stages method

The successive stages method (or mixed cells in series model or cascade of perfectly mixed tanks) (Fig. 2), is a widely used method for the solution of separation processes, see, for example (Coker, Allen, Freeman, & Fleming, 1999; Coker et al., 1998), in the case of membrane permeation, Cheng and Hill (1985) in the case of pressure swing adsorption and Charton and Nicoud (1995) and Ludemann-Hombourger et al. (2000) in the case of simulated moving bed.

The equivalent total mass balance equation using the successive stages method is given by the following equation:

$$\frac{\partial c_T^k}{\partial \theta} = -n(u^k c_T^k - u^{k-1} c_T^{k-1}) - \sum_{i=1}^{nc} N_i^k, \quad k = 1, n \tag{16}$$

where n is the number of stages. The ith component mass balance is given by:

$$\frac{\partial c_i^k}{\partial \theta} = -n(u^k c_i^k - u^{k-1} c_i^{k-1}) - N_i^k \tag{17}$$

And the pressure drop equation is given by:

$$u^k = -n\left(\frac{p_T^{k+1} - p_T^k}{\beta}\right) \tag{18}$$

where $c_T^k = \sum_{i=1}^{nc} c_i^k$, $c_T^k = p_T^k / T^k$.

3.1. Velocity profile in diluted systems

In diluted systems, the total mass balance equation should not be solved, since the velocity profile can be considered constant:

$$u^k = u_{in}, \quad \text{for } k = 1, n \tag{19}$$

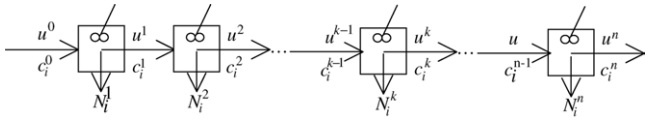

Fig. 2. Successive stages method applied to a separation process.

3.2. Velocity profile without pressure drop (isothermal)

Boundary conditions: $\partial c_T/\partial\theta = c_T^\theta$ and $u_0 = u_{in}$. The velocity profile is calculated by the following equation:

$$u^k = u^{k-1} - \frac{1}{nc_T}\left(c_T^\theta + \sum_{i=1}^{nc} N_i^k\right), \quad k = 1, n \tag{20}$$

Boundary conditions: $\partial c_T/\partial\theta = c_T^\theta$ and $u^n = u_{out}$. The velocity profile is calculated by the following equations:

$$u^0 = 0, \qquad u^k = u^{k-1} - \frac{1}{nc_T}\left(c_T^\theta + \sum_{i=1}^{nc} N_i^k\right),$$

$$k = 1, \ldots, n, \qquad \gamma = u_{out} - u^n, \qquad u^k = u^k + \gamma,$$

$$k = 1, \ldots, n \tag{21}$$

Boundary conditions: $u^0 = u_{in}$ and $u^n = u_{out}$. The velocity profile is calculated by the following equations:

$$c_T^\theta = -c_T(u_{out} - u_{in}) + \sum_{k=1}^{n}\sum_{i=1}^{nc}(N_i^k \Delta x^k) \tag{22}$$

$$u^k = u^{k-1} - \frac{1}{nc_T}\left(c_T^\theta + \sum_{i=1}^{nc} N_i^k\right), \quad k = 1, n-1 \tag{23}$$

3.3. Velocity profile with pressure drop (non-isothermal)

The velocity profile is calculated by the following equation:

$$u^k = -n\left(\frac{p_T^{k+1} - p_T^k}{\beta}\right) \tag{24}$$

Boundary conditions: $p_T^0 = p_{T,in}$ and $p_T^n = p_{T,out}$

$$u_{in} = -\frac{2n}{\beta}(p_T^1 - p_{T,in}) \tag{25}$$

$$u_{out} = -\frac{2n}{\beta}(p_{T,out} - p_T^n) \tag{26}$$

Boundary conditions: $u_0 = u_{in}$ and $u^n = u_{out}$:

$$p_{T,in} = \frac{\beta}{2n}u_{in} + p_T^1 \tag{27}$$

$$p_{T,out} = p_T^n - \frac{\beta}{2n}u_{out} \tag{28}$$

The pressure profile is calculated by the integration of the following equation:

$$\frac{\partial c_T^k}{\partial\theta} = -n\left(u^k c_T^k - u^{k-1}c_T^{k-1}\right) - \sum_{i=1}^{nc} N_i^k, \quad k = 1, n \tag{29}$$

4. Finite volume method

In finite volume method the values of the conserved variables (for example: molar concentration) are averaged across the volume and the conservation principle is always assured. This is the reason why it has been successfully used for heat transfer and mass flow problems.

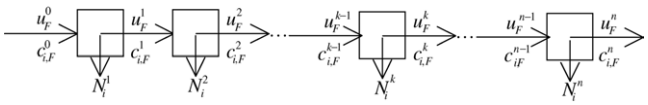

Fig. 3. Finite volume method applied to a separation process.

Fig. 3 presents the finite volume discretization method in a schematic form. u_F^k is the velocity in the face k and $c_{F,i}^k$ the concentration of i species in the face k.

The equivalent total mass balance equation using the finite volume method is given by the following equation:

$$\frac{\partial \widehat{c}_T^k}{\partial\theta} = -\frac{u_F^k c_{T,F}^k - u_F^{k-1}c_{T,F}^{k-1}}{\Delta x^k} - \sum_{i=1}^{nc}\widehat{N}_i^k, \quad k = 1, n \tag{30}$$

where Δx^k is the volume in k stage. And the partial mass balance is given by:

$$\frac{\partial \widehat{c}_i^k}{\partial\theta} = \frac{1}{Pe}\frac{c_{T,F}^k(c_i^k/c_T^k)'_F - c_{T,F}^{k-1}(c_i^{k-1}/c_T^{k-1})'_F}{\Delta x^k} - \frac{u_F^k c_{i,F}^k - u_F^{k-1}c_{i,F}^{k-1}}{\Delta x^k} - \widehat{N}_i^k \tag{31}$$

$\widehat{c}_i^k$ is the cell average concentration that is a function of c_i^k as it follows (Leonard, 1995):

$$\widehat{c}_i^k = c_i^k + \frac{(\Delta x^k)^2}{24}(c_i^k)'' + \frac{(\Delta x^k)^4}{1920}(c_i^k)^{(iv)} + \cdots \tag{32}$$

$(c_i^k/c_T^k)'_F$ is the derivative of (c_i^k/c_T^k) in the face k and is a function of the neighboring cells. Using a second-order approximation (central difference scheme—CDS2) we obtain:

$$(c_i^k/c_T^k)'_F = \frac{(c_i^{k+1}/c_T^{k+1}) - (c_i^k/c_T^k)}{(1/2)(\Delta x^{k+1} + \Delta x^k)} \tag{33}$$

$c_{i,F}^k$ is the concentration of species i in the face k and is a function of the neighboring cells, as follows:

$$c_{i,F}^k = f(c_i^{k-1}, c_i^k, c_i^{k+1}, c_i^{k+2}) \quad \text{and} \quad c_{T,F}^k = \sum_{i=1}^{nc} c_{i,F}^k \tag{34}$$

Several methods have been proposed in the literature for the calculation of $c_{i,F}^k$ (concentration of species i in the face k), such as the first-order upwind differencing scheme (UDS) of Courant el al. (1952), $c_{i,F}^k = c_i^k$, $i = 1, \ldots$, nc, the second-order linear upwind scheme (LUDS) of Shyy (1985), $c_{i,F}^k = \frac{3}{2}c_i^k - \frac{1}{2}c_i^{k-1}$, $i = 1, \ldots$, nc, or the third-order QUICK scheme of Leonard (1979), $c_{i,F}^k = \frac{1}{2}(c_i^{k+1} + c_i^k) - \frac{1}{8}(c_i^{k+1} + 2c_i^k + c_i^{k-1})$, $i = 1, \ldots$, nc, which are all upwind biased. Central schemes are often used, such as the second-order central (CDS2), $c_{i,F}^k = \frac{1}{2}(c_i^{k+1} + c_i^k)$, $i = 1, \ldots$, nc, or the fourth-order central differences (CDS4). All these methods, with the exception of the first-order UDS, suffer from lack of boundedness and, for highly convective flows, the occurrence of unphysical oscillations is usual. Two different bounded approaches are nowadays commonly used:

high-resolution schemes (HRS) and weighted essentially non-oscillatory (WENO) schemes. These are, by definition, bounded higher-order schemes and will be briefly described below.

4.1. Velocity profile in diluted systems

In diluted systems, the total mass balance equation should not be solved, because the velocity profile can be considered constant:

$$u_{\mathrm{F}}^0 = u^0 \tag{35}$$

4.2. Velocity profile without pressure drop (isothermal)

Boundary conditions: $\partial c_{\mathrm{T}}/\partial\theta = c_{\mathrm{T}}^{\theta}$ and $u_{\mathrm{F}}^0 = u_{\mathrm{in}}$. The velocity profile is calculated by the following equation:

$$u_{\mathrm{F}}^k = u_{\mathrm{F}}^{k-1} - \frac{\Delta x^k}{c_{\mathrm{T}}}\left(c_{\mathrm{T}}^{\theta} + \sum_{i=1}^{\mathrm{nc}} N_i^k\right), \quad k = 1, n \tag{36}$$

Boundary conditions: $\partial c_{\mathrm{T}}/\partial\theta = c_{\mathrm{T}}^{\theta}$ and $u^n = u_{\mathrm{out}}$. The velocity profile is calculated by the following equations:

$$u_{\mathrm{F}}^0 = 0, \qquad u_{\mathrm{F}}^k = u_{\mathrm{F}}^{k-1} - \frac{\Delta x^k}{c_{\mathrm{T}}}\left(c_{\mathrm{T}}^{\theta} + \sum_{i=1}^{\mathrm{nc}} N_i^k\right),$$

$$k = 1, \ldots, n, \qquad \gamma = u_{\mathrm{out}} - u_{\mathrm{F}}^n, \qquad u_{\mathrm{F}}^k = u_{\mathrm{F}}^k + \gamma,$$

$$k = 1, \ldots, n \tag{37}$$

Boundary conditions: $u_{\mathrm{F}}^0 = u_{\mathrm{in}}$ and $u_{\mathrm{F}}^n = u_{\mathrm{out}}$. The velocity profile is calculated by the following equations:

$$c_{\mathrm{T}}^{\theta} = \sum_{k=1}^{n}\sum_{i=1}^{\mathrm{nc}}(N_i^k \Delta x^k) - c_{\mathrm{T}}(u_{\mathrm{out}} - u_{\mathrm{in}}) \tag{38}$$

$$u_{\mathrm{F}}^k = u_{\mathrm{F}}^{k-1} - \frac{\Delta x^k}{c_{\mathrm{T}}}\left(c_{\mathrm{T}}^{\theta} + \sum_{i=1}^{\mathrm{nc}} N_i^k\right), \quad k = 1, n-1 \tag{39}$$

4.3. Velocity profile with pressure drop (non-isothermal)

Using a second-order approximation (CDS2), the pressure drop equation is given by:

$$u_{\mathrm{F}}^k = -\frac{2}{\beta}\frac{p_{\mathrm{T}}^{k+1} - p_{\mathrm{T}}^k}{\Delta x^{k+1} + \Delta x^k} \tag{40}$$

where

$$c_{\mathrm{T}}^k = \sum_{i=1}^{\mathrm{nc}} c_i^k, \qquad c_{\mathrm{T}}^k = \frac{p_{\mathrm{T}}^k}{T^k} \tag{41}$$

Boundary conditions: $p_{\mathrm{T,F}}^0 = p_{\mathrm{T,in}}$ and $p_{\mathrm{T,F}}^n = p_{\mathrm{T,out}}$

$$u_{\mathrm{F}}^0 = u_{\mathrm{in}} = -\frac{2}{\beta}\frac{p_{\mathrm{T}}^1 - p_{\mathrm{T,F}}^0}{\Delta x^1} \tag{42}$$

$$u_{\mathrm{F}}^n = u_{\mathrm{out}} = -\frac{2}{\beta}\frac{p_{\mathrm{T,F}}^n - p_{\mathrm{T}}^n}{\Delta x^n} \tag{43}$$

Boundary conditions: $u_{\mathrm{F}}^0 = u_{\mathrm{in}}$ and $u_{\mathrm{F}}^n = u_{\mathrm{out}}$:

$$p_{\mathrm{T,in}} = \frac{\beta\Delta x^1}{2}u_{\mathrm{in}} + p_{\mathrm{T,F}}^1 \tag{44}$$

$$p_{\mathrm{T,out}} = p_{\mathrm{T,F}}^n - \frac{\beta\Delta x^n}{2}u_{\mathrm{out}} \tag{45}$$

The equations presented for the boundaries (44) and (45) are only first-order accurate. That should not be a problem in common separation problems. However for processes with high pressure drop these equations should be replaced by at least a second-order accurate approximation.

5. HRS and WENO schemes

As mentioned before, the application of conventional higher-order discretization schemes to the advective term (convection term) of hyperbolic or parabolic equations dominated by convection is not adequate, due to the occurrence of non-physical oscillations.

In order to overcome this issue, an extensive amount of research has been directed towards the development of accurate and bounded non-linear convective schemes. Several discretization schemes were proposed on the total variation-diminishing framework (TVD) (Harten, 1983; Shyy, 1985) and more recently on the normalized variable formulation (NVF) (Leonard, 1987) and its extension, the normalized variable and space formulation (NVSF) of Darwish and Moukalled (1994).

Considering a general grid, as illustrated in Fig. 4. The labeling of the nodes depends on the local velocity, u_{F}, calculated at face F. For a given face F, the U and D nodes refer to the upstream and downstream points, relative to node P, which is itself upstream to the face F under consideration, as shown in Fig. 4.

According to the NVSF, the face values are interpolated as (Darwish and Moukalled, 1994):

$$y_{\mathrm{F}} = y_{\mathrm{U}} + \tilde{y}_{\mathrm{F}}(y_{\mathrm{D}} - y_{\mathrm{U}}) \tag{46}$$

where y is the convected variable (for example c_i).

The normalized face value, $\tilde{y}_{\mathrm{F}}$, is calculated using an appropriate non-linear limiter. As a example we present the SMART (Gaskell & Lau, 1988) limiter (third-order convergence in smooth regions):

$$\tilde{y}_{\mathrm{F}} = \max\left[\tilde{y}_{\mathrm{P}}, \min\left(\frac{\tilde{x}_{\mathrm{F}}(1 - 3\tilde{x}_{\mathrm{P}} + 2\tilde{x}_{\mathrm{F}})}{\tilde{x}_{\mathrm{P}}(1 - \tilde{x}_{\mathrm{P}})}\tilde{y}_{\mathrm{P}}, \frac{\tilde{x}_{\mathrm{F}}(1 - \tilde{x}_{\mathrm{F}})}{\tilde{x}_{\mathrm{P}}(1 - \tilde{x}_{\mathrm{P}})}\tilde{y}_{\mathrm{P}} + \frac{\tilde{x}_{\mathrm{F}}(\tilde{x}_{\mathrm{F}} - \tilde{x}_{\mathrm{P}})}{1 - \tilde{x}_{\mathrm{P}}}, 1\right)\right] \tag{47}$$

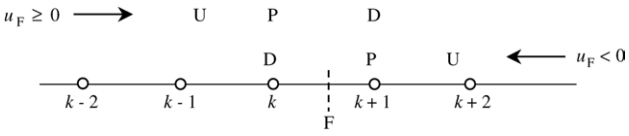

Fig. 4. Definition of local variables.

and the MINMOD limiter (Harten, 1983) (second-order convergence in smooth regions):

$$\tilde{y}_F = \max\left[\tilde{y}_P, \min\left(\frac{\tilde{x}_F}{\tilde{x}_P}\tilde{y}_P, \frac{1-\tilde{x}_F}{1-\tilde{x}_P}\tilde{y}_P + \frac{\tilde{x}_F - \tilde{x}_P}{1-\tilde{x}_P}\right)\right] \quad (48)$$

where the normalized variables $\tilde{y}_P$, $\tilde{x}_P$ and $\tilde{x}_F$ are calculated using:

$$\tilde{y}_P = \frac{y_P - y_U}{y_D - y_U}, \qquad \tilde{x}_P = \frac{x_P - x_U}{x_D - x_U}, \qquad \tilde{x}_F = \frac{x_F - x_U}{x_D - x_U} \quad (49)$$

More details on this issue, and other high-resolution schemes, can be found in the works of Darwish and Moukalled (1994) and Alves, Oliveira, and Pinho (2003).

According to the third-order WENO scheme, the face fluxes are interpolated as (Shu, 1997; Shu & Osher, 1988, 1989):

$$y_F = w_0 y_F^0 + w_1 y_F^1 \quad (50)$$

with $y_F^0 = \frac{1}{2}(y_D + y_P)$ (CDS2), $y_F^1 = \frac{3}{2}y_P - \frac{1}{2}u_U$ (LUDS) and w_i defined by:

$$w_j = \frac{\alpha_j}{\alpha_0 + \alpha_1}, \qquad \alpha_j = \frac{d_j}{(\varepsilon + \beta_j)^2}, \quad j = 0, 1 \quad (51)$$

where $\varepsilon > 0$ is introduced to avoid the denominator became zero. We take $\varepsilon = 1 \times 10^{-6}$ in all our numerical tests. The smoothness measurement is defined by:

$$\beta_0 = (y_D - y_P)^2, \qquad \beta_1 = (y_P - y_U)^2 \quad (52)$$

and $d_0 = \frac{2}{3}$ and $d_1 = \frac{1}{3}$.

6. Temporal integration

The time integration of the resulting system of ordinary differential equations (ODEs initial value problem) can be accomplished using solver LSODA (Petzold, 1983). This routine solves initial boundary problems for stiff or non-stiff systems of first-order ODEs. For non-stiff systems, it makes use of the Adams method with variable order (up to 12th order) and step size, while for stiff systems it uses the Gear (or BDF) method with variable order (up to 5th order) and step size. In our test cases the error in time integration was always set small enough to ensure that the numerical errors are mainly due to inaccuracies in spatial discretization.

7. Application examples

7.1. Steady-state membrane permeation processes

The use of membrane technology in gas separation has grown significantly in the last decades due to the development of highly selective materials and the lower power consumptions involved (Mendes et al., 2003). The hollow-fibber membrane separation is based on the different permeability coefficients of each component through a selective barrier, porous or non-porous (dense).

Several models have been developed along the last years for the simulation and optimization of a membrane permeation module. An extensive revision is presented by Kovvali, Vemury, Krovvidi, and Khan (1992). The analytical solution of mass and momentum balance equations can only be obtained under some assumptions. Weller and Steiner (1950) present an analytical solution, based on the following assumptions: plug-flow pattern, constant and composition independent permeability and negligible pressure drop and Smith, Hall, Freeman, and Rautenbach, 1996 assuming perfectly mixed pattern in the permeate side.

The numerical solution can be obtained using series approximations and numerical methods applied to the solution of ordinary differential equations. Kovvali et al. (1992) and Boucif, Majumdar, and Sirkar (1984) present models for binary mixtures and Pettersen and Lien (1994) and Chang, Min, Oh, and Moon (1998) for multicomponent mixtures using series approximations. Kovvali et al. (1992), Pan (1983) and Chen, Li, and Teo (1995) have solved the model equations using the shooting method, which consists in solving the boundary conditions problem as an initial condition problem, with an iteration strategy. This approach is not very efficient and the convergence is not always assured.

Kaldis, Kapantaidakis, Papadopoulos, and Sakellaropoulos (1998) and Tessendorf, Gani, and Michelsen, 1999 have used the orthogonal collocation method for solving the model equations. This strategy conduces to a system of non-linear equations which convergence is very dependent on the estimated composition profile. Coker et al. (1999, 1998) and Thundyil and Koros (1997) have solved the model equations using the successive stages method (upwind differencing scheme). The system of equations obtained in the case of constant permeability is linear, and so it can be solved very efficiently. However, a higher number of mesh points is necessary, i.e. 100–1000, see (Coker et al., 1998), for obtaining an accurate solution, which conduces to a higher memory consumption, namely in multicomponent systems.

The numerical solution of permeation models has three important issues that should be discussed: the convergence of the non-linear system of equations that results from the discretization of the ordinary differential equations, the treatment of boundary conditions and the accuracy of the discretization scheme.

The discretization of the model equations using high order schemes conduces to a system of non-linear algebraic equations. The solution of this system using, for example, the Newton–Raphson method converges to the exact solution only if a good initial guess is used. The solution of the problem in non-steady-state, as proposed, eliminates this problem.

The treatment of boundary conditions is also an important issue. The main problem occurs when solving the ordinary differential equation for the permeate side with no purge, using finite difference methods. In this case the concentration in $x = 0$ (cocurrent pattern) or $x = 1$ (countercurrent pattern) is not known, and should be estimated based on the retentate/permeate conditions. This problem does not occur when using the successive stages method and the finite volume method.

The discretization scheme used is the final important issue that should be pointed out. The successive stages method is a first-order accurate method and therefore it is not recommended, as will be seen in the following illustration examples.

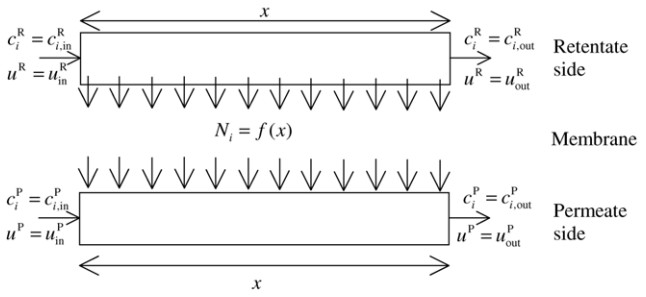

Fig. 5. Sketch of the model proposed for the solution of membrane permeation problems.

7.1.1. Mass exchange

The mass exchanged between the retentate and permeate, considering that the resistance to the mass transfer is only imposed by the selective barrier, and that the membrane does not have any defect and permeability coefficient is constant, can be written as follows:

$$N_i = \frac{A_T}{A_S} L_i \frac{p_i^R - p_i^P}{\delta_F} \tag{53}$$

where L_i is the species i permeability coefficient, δ_F the membrane thickness, A_T mass exchange perimeter and A_S the flow section area. The subscripts R and P mean retentate and permeate side, respectively.

7.1.2. Boundary conditions

Following we present the boundary conditions for different flow patterns and $1/Pe = 0$ (Fig. 5):

- Cocurrent flow without recycle
  - Retentate
    $x = 0: \quad u^R = u_{in}^R, \; y_i^R = y_{i,in}^R;$
    $x = 1: \quad p_T^R = p_{T,out}^R$
  - Permeate
    $x = 0: \quad u^P = 0; \qquad x = 1: \quad p_T^P = p_{T,out}^P$
- Cocurrent flow with recycle/purge
  - Retentate
    $x = 0: \quad u^R = u_{in}^R, \quad y_i^R = y_{i,in}^R;$
    $x = 1: \quad p_T^R = p_{T,out}^R$
  - Permeate
    $x = 0: \quad u^P = u_{in}^P, \quad y_i^P = y_{i,in}^P;$
    $x = 1: \quad p_T^P = p_{T,out}^P$
- Countercurrent flow without recycle
  - Retentate
    $x = 0: \quad u^R = u_{in}^R, \quad y_i^R = y_{i,in}^R;$
    $x = 1: \quad p_T^R = p_{T,out}^R$
  - Permeate
    $x = 1: \quad u^P = 0; \qquad x = 0: \quad p_T^P = p_{T,out}^P$

Table 1
Permeance and feed composition for air separation simulations (Coker et al., 1998)

Component	Feed mole fraction	Permeability coefficient (GPU)[a]
N_2	0.7841	3.57
O_2	0.2084	20
CO_2	0.0003	60
H_2O	0.0072[b]	1000

[a] 1 GPU = 3.346×10^{-13} kmol/m^2 s Pa.
[b] The water composition corresponds to saturation at 40 °C and 10 atm total pressure.

7.1.3. Results and discussion

The simulations results described in this section are for countercurrent contacting. We present as test case the air separation in a polysulfone membrane. The permeances of the membrane to air gas components are presented in Table 1. The membrane permeances are selected to be similar to those which might be observed with a polysulfone membrane with an effective separating layer thickness of approximately 0.1 μm (Coker et al., 1998).

Fig. 6 presents the simulation results for countercurrent contacting without recycle. The effect of mesh refinement in the nitrogen purity is shown as a function of overall residue recovery (stage cut). Fig. 6a concerns the results obtained using QUICK

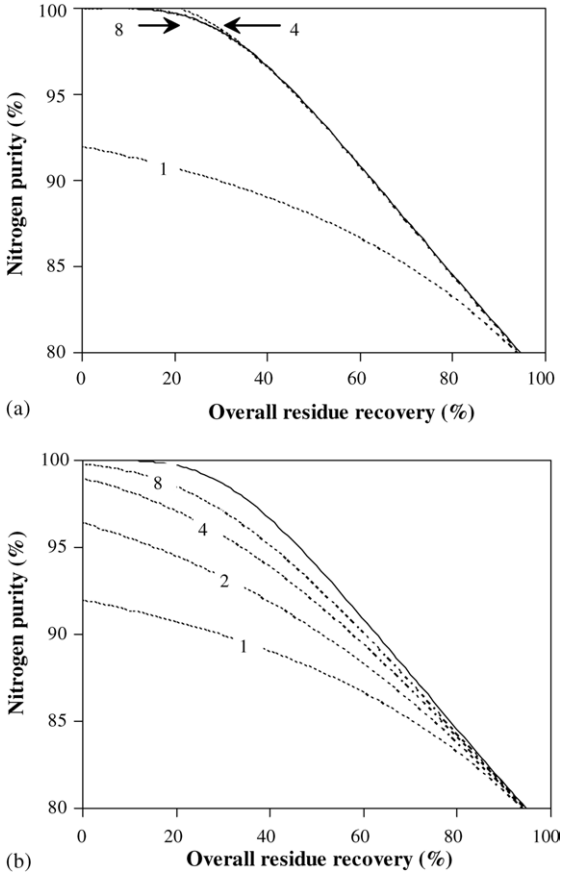

Fig. 6. Effect of mesh refinement on nitrogen purity in retentate ($p_T^R/p_T^P = 5$): (···) $n = 1, 2, 4, 8$, (—) reference solution. (a) QUICK scheme and (b) UDS scheme (successive stages method).

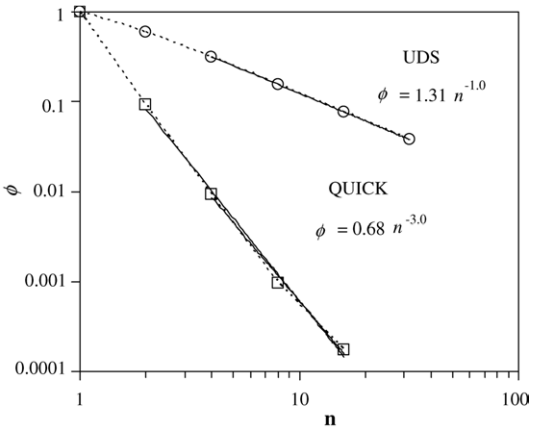

Fig. 7. Effect of mesh refinement on nitrogen purity in retentate ($p_T^R/p_T^P = 5$): QUICK scheme and UDS scheme (successive stages method).

discretization scheme and Fig. 6b concerns the results obtained using the successive stages method (Coker et al., 1998).

With the proposed method it is possible to obtain an acceptable solution with only eight discretization volumes for all values of overall residue recovery. The successive stages method converges slowly to the reference solution, namely for high values of stage cut. Coker et al. (1998) mentions that in some cases, when the stage cut is extremely high (>90%), at least 1000 stages are required to obtain the problem solution.

Fig. 7 presents the error of the solution, ϕ, as a function of the number of stages/discretization volumes. In this figure, ϕ is defined as follows:

$$\phi = \frac{|\mathrm{Pur_R} - \mathrm{Pur}_i|}{|\mathrm{Pur_R} - \mathrm{Pur_{one\,stage}}|} \tag{54}$$

where $\mathrm{Pur_R}$ is the reference value of purity in the retentate, $\mathrm{Pur_{one\,stage}}$ the purity in the retentate obtained using one stage, and Pur_i the purity obtained using i stages (discretization volumes). From Fig. 7 it is possible to see that UDS (successive stages method) converges to the reference solution with only first-order accuracy and the QUICK scheme converges approximately with third-order accuracy. For obtaining a solution with an accuracy equivalent to eight volumes using the QUICK scheme it is necessary to use 1000 successive stages. And for obtaining a solution with an accuracy equivalent to 16 volumes using QUICK scheme it is necessary to use 7800 successive stages.

From this simple example and analysis, it can be seen that the successive stages method should not be used for high stage-cut values and/or multicomponent mixtures, due to the high number of equations that need to be solved.

We have tested some other high-resolution schemes, namely the SMART scheme, MINMOD scheme and the third-order WENO scheme. The results obtained using SMART scheme are identical to the ones obtained using QUICK scheme. This seems to be obvious since the SMART scheme uses QUICK scheme in smooth regions (note that the problem presented is always smooth), the MINMOD and third-order WENO present, with mesh refinement, only a second-order convergence. In the case of non-smooth problems (high convective problems) QUICK scheme conduces to the appearance of non-physical oscillations in the solution, and so the SMART scheme is recommended.

As a conclusion on this topic, we should remark two aspects. A correct implementation of the finite volume method as it was presented, using a third-order accurate approximation (as QUICK scheme), conduces to accurate solutions with a modest number of mesh points (discretization volumes). The local and global flux conservation, that is intrinsic to the finite volume method, is a key issue to the success of the method.

7.2. Cyclic adsorption processes

Cyclic adsorption processes are based on the selective retention (based on adsorption equilibrium selectivity or diffusion selectivity) of one or more components in a gas mixture, with the adsorbent regeneration being performed by total or partial pressure decrease (pressure swing adsorption—PSA, vacuum swing adsorption—VSA or vacuum pressure swing adsorption—VPSA) or by temperature increase (temperature swing adsorption—TSA). These processes are intrinsically dynamic, operating in a periodic fashion with a fixed (or variable) period.

The models of cyclic adsorption processes can only be solved analytically in the case of purifications, using the method of characteristics, under the following ideal conditions (Knaebel & Hill, 1985; Shendalm & Mitchell, 1972): isothermal system, instantaneous equilibrium between the gaseous phase and the adsorbed phase, negligible pressure drop, linear isotherm and frozen concentration profile during pressurization and depressurization stages. In the case of separations, the assumptions mentioned before are not usually valid, and so the system of partial differential equations must be solved numerically.

Usually, in cyclic adsorption processes simulation, one of the following strategies is applied to solve the model equations. The first one consists in the simultaneous space and time discretization and posterior resolution of the resulting non-linear algebraic system of equations, for example: double collocation (Raghavan & Ruthven, 1985) and space and time finite differences (Cen & Yang, 1985; Yang & Lee, 1998). The other strategy consists in the spatial discretization and subsequent integration of the resulting initial value system of ordinary differential equations (ODE) with an appropriate integrator (Finlayson, 1992): method of lines (MOL). Normally the integrator used is based on the BDF (backward differentiation formulas), known as Gear formulas (Gear, 1971), that are suitable for the solution of stiff problems (Byrne et al., 1977; Hindmarsh, 1974; Petzold, 1983) or Runge–Kutta Fehlberg method (RKF45—Fehlberg, 1968) that is unsuitable for the solution of stiff problems but commonly used in cyclic adsorption processes simulation.

Different numerical methods have been applied to the solution of cyclic adsorption processes using the method of lines: successive stages method (Cheng & Hill, 1985), orthogonal collocation (Arvind, Farooq, & Ruthven, 2002; Raghavan, Hassan, & Ruthven, 1985), finite differences (Ko & Moon, 2000), orthogonal collocation on finite elements (Da Silva,

Silva, & Rodrigues, 1999), Galerkin finite elements (Teague & Edgar, 1999). The use of high-resolution schemes has been mentioned in the work of Cruz et al. (2003).

In a kinetic based separation, the method used in spatial discretization is not fundamental in order to obtain an accurate solution, since the problem does not normally involve a sharp moving front. In this case, the orthogonal collocation and Galerkin methods are usually better than the others, as they have a higher convergence. However, in an equilibrium based separation, which is the most common separation type, the appropriate choice of discretization method is fundamental in order to obtain an accurate solution. In this case, the problem involves a sharp moving front, which is steeper as the selectivity increases and/or the dispersive effects (mass transfer resistance, for example) decrease. The use of bounded methods, as the successive stages approximation, is important in order to obtain stable solutions without oscillations in the computation domain. The appearance of oscillations in cyclic adsorption process simulation could conduce to a divergence in the integrator as well as mathematical impossibility when calculating the adsorption equilibrium concentration.

The use of high-resolution schemes conduces always to stable solutions with a high convergence to the reference solution, as will be seen in the following examples.

7.2.1. Mass exchange rate

In cyclic adsorption processes the mass exchange rate between the particle and its surroundings is normally given by the following expression:

$$N_i = \frac{1-\varepsilon_b}{\varepsilon_b}\left[\varepsilon_p \frac{\partial \bar{c}_i}{\partial t} + \rho_s \frac{\partial \bar{q}_i}{\partial t}\right] \tag{55}$$

where ε_b is the bed void fraction (ratio between the free volume and the total volume), ε_p the particle porosity, $\bar{q}_i$ the average molar concentration in the adsorbed phase and $\bar{c}_i$ the molar average concentration in the fluid phase.

7.2.2. Intra-particle mass transfer

Different approximations can be considered for describing the intra-particle mass transfer. In this work we use the linear driving force (LDF) approximation (Glueckauf, 1955), assuming instantaneous equilibrium between the inter-particle gas phase and the intra-particle gas phase ($\partial \bar{c}_i^*/\partial\theta = \partial c_i^*/\partial\theta$). This model can be derived from the intra-particle mass balance equation, which is a partial differential equation, considering parabolic profile inside the particle (Liaw, Wang, Greenkorn, & Chao, 1979):

$$\frac{\mathrm{d}\bar{q}_i}{\mathrm{d}\theta} = k_i(q_{i,s} - \bar{q}_i) \quad \text{and} \quad \frac{\partial \bar{c}_i}{\partial \theta} = \frac{\partial c_i}{\partial \theta} \tag{56}$$

where k_i is the LDF coefficient, $k_i = 15 D^e_{i,M}/r_p^2$, $D^e_{M,i}$ the effective homogeneous diffusion coefficient, r_p the particle radius, $q_{i,s}$ the molar concentration in the particle surface (adsorbed phase) that is related with the molar concentration in the inter-particle gas phase through the adsorption equilibrium isotherm:

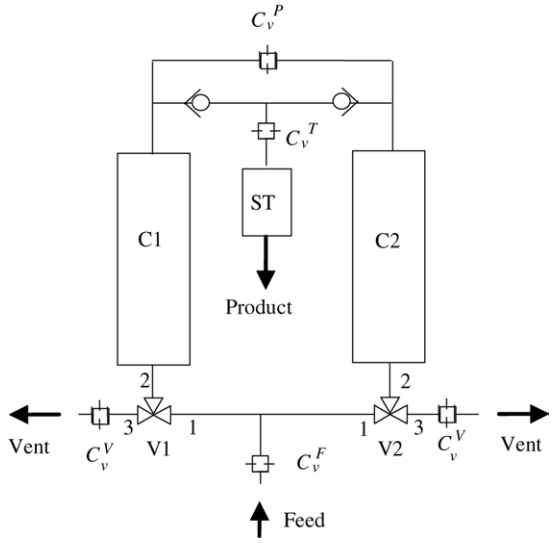

Fig. 8. Sketch of a small pressure swing adsorption unit.

$q_{i,s} = f(p_r, p_i)$. In dimensionless form:

$$\frac{\mathrm{d}\bar{q}_i^*}{\mathrm{d}\theta} = \varphi\alpha_{i,M}(q_{i,s}^* - \bar{q}_i^*) \tag{57}$$

where $\varphi = \tau_b k_{ref}$ and $\alpha_{i,M} = D^e_{i,M}/D_{ref} = k_i/k_{ref}$. The subscript "ref" means reference condition.

7.2.3. Boundary conditions

Cyclic adsorption processes are intrinsically dynamic, operating in a periodic fashion, and so the boundary conditions change with time. In this work we propose the study of a small pressure swing adsorption unit as described by Santos et al. (2004).

Fig. 8 presents a sketch of this unit.

Since there are no valves to control the duration of pressurization, this step depends on the difference between the pressure inside the storage tank (ST in Fig. 8) and inside the adsorption column. Due to the use of check valves, production will start when the pressure inside the columns is higher than inside the product tank.

The unit can operate at two different stages: stage 1 where pressurization and production take place, and stage 2 where the column is depressurized and purged. Table 2 presents the position of the three-way valves in the base of the columns for each stage.

When column 1 is pressurizing/producing and column 2 is depressurizing/ purging the boundary conditions in the dimensionless form are (for the sake of simplicity the superscript "*" was omitted):

Table 2
Flow direction at each valve for each step

	Stage 1	Stage 2
V1	1 → 2	2 → 3
V2	2 → 3	1 → 2

- Column 1

$$x = 0: \quad \frac{1}{Pe}\frac{\partial y_i}{\partial x} = u_{\text{in}}(y_i - y_{i,\text{in}}) \tag{58}$$

$$u = \frac{C_{\text{v}}^{\text{F}}}{p_{\text{T}}^{1}} f(p_{\text{T}}^{\text{H}}, p_{\text{T}}^{1}, T, M) \tag{59}$$

$$x = 1: \quad \begin{cases} \dfrac{\partial y_i}{\partial x} = 0, & p_{\text{T}}^{1} \geq p_{\text{T}}^{2} \\ \dfrac{1}{Pe}\dfrac{\partial y_i}{\partial x} = u(y_i - y_i|_{x=1,\text{column 2}}), & p_{\text{T}}^{1} < p_{\text{T}}^{2} \end{cases} \tag{60}$$

$$u = \frac{C_{\text{v}}^{\text{P}}}{p_{\text{T}}^{1}} f(p_{\text{T}}^{1}, p_{\text{T}}^{2}, T^*, M) + \frac{u_{\text{in}}^{\text{ST}} p_{\text{T}}^{\text{ST}}}{\varepsilon_{\text{b}} p_{\text{T}}^{1}}, \quad p_{\text{T}}^{1} \geq p_{\text{T}}^{2},$$

$$u = -\frac{C_{\text{v}}^{\text{P}}}{p_{\text{T}}^{1}} f(p_{\text{T}}^{2}, p_{\text{T}}^{1}, T, M), \quad p_{\text{T}}^{1} < p_{\text{T}}^{2} \tag{61}$$

Eq. (59) can be replaced by a correlation that relates the flow rate given by a compressor with the pressure inside the adsorption column.

- Column 2

$$x = 0: \quad \frac{\partial y_i}{\partial x} = 0 \tag{62}$$

$$u = -\frac{C_{\text{v}}^{\text{V}}}{p_{\text{T}}^{2}} f(p_{\text{T}}^{2}, p_{\text{T}}^{\text{L}}, T, M) \tag{63}$$

$$x = 1: \quad \begin{cases} \dfrac{\partial y_i}{\partial x} = 0, & p_{\text{T}}^{2} \geq p_{\text{T}}^{1} \\ \dfrac{1}{Pe}\dfrac{\partial y_i}{\partial x} = u(y_i - y_i|_{x=1,\text{column 1}}), & p_{\text{T}}^{2} < p_{\text{T}}^{1} \end{cases} \tag{64}$$

$$u = -\frac{C_{\text{v}}^{\text{P}}}{p_{\text{T}}^{2}} f(p_{\text{T}}^{1}, p_{\text{T}}^{2}, T, M), \quad p_{\text{T}}^{1} \geq p_{\text{T}}^{2},$$

$$u = \frac{C_{\text{v}}^{\text{P}}}{p_{\text{T}}^{2}} f(p_{\text{T}}^{2}, p_{\text{T}}^{1}, T, M) + \frac{u_{\text{in}}^{\text{ST}} p_{\text{T}}^{\text{ST}}}{\varepsilon_{\text{b}} p_{\text{T}}^{2}}, \quad p_{\text{T}}^{1} < p_{\text{T}}^{2} \tag{65}$$

where the dimensionless average molar velocity of the stream entering the storage tank, $u_{\text{in}}^{\text{ST}}$, is given by:

$$u_{\text{in}}^{\text{ST}} p_{\text{T}}^{\text{ST}} = C_{\text{v}}^{\text{ST}} f(p_{\text{T}}, p_{\text{T}}^{\text{ST}}, T, M) \tag{66}$$

The molar velocity across a valve orifice was described by (Chou & Huang, 1994; Teague & Edgar, 1999):

$$up = C_{\text{v}} f(p_{\text{u}}, p_{\text{d}}, T, M) \tag{67}$$

where C_{v} is the valve parameter given by:

$$C_{\text{v}} = 2.035 \times 10^{-2} \frac{T_{\text{ref}}}{\varepsilon_{\text{b}} A u_{\text{ref}} \sqrt{p_{\text{ref}}}} \frac{p^0}{T^0} K_{\text{v}} \tag{68}$$

Table 3
Adsorption equilibrium isotherm parameters (Santos et al., 2004)

	N_2	O_2	Ar
$q_{\max}$ (mol/kg)	3.0704	3.0704	3.0704
b_i ($\times 10^5$ Pa^{-1})	0.1015	0.0369	0.0340
$\Delta H/\Re$ (K)	1767	2501	1791

and

$$f(p_{\text{u}}, p_{\text{d}}, T, M) = \begin{cases} 1.179\sqrt{\dfrac{p_{\text{u}}^2 - p_{\text{d}}^2}{p_{\text{d}} M}}\, T, & p_{\text{d}} > 0.53 p_{\text{u}} \\ p_{\text{u}}\sqrt{\dfrac{1}{p_{\text{d}} M}}\, T, & p_{\text{d}} \leq 0.53 p_{\text{u}} \end{cases} \tag{69}$$

where K_{v} is the valve parameter, p_{u} and p_{d} are the dimensionless upstream and downstream pressures, respectively, T the dimensionless temperature and M the molecular weight of the gas passing through the orifice. The superscript "0" stands for standard temperature and pressure conditions (STP).

7.2.4. Results and discussion

The simulations were performed for the oxygen production from air (nitrogen, 78%; oxygen, 21%; argon, 1%) using the 13X zeolite type Oxysiv 5 from UOP. The cycles optimized were the ones of the oxygen concentrator and of the small PSA unit presented in Santos et al. (2004). The single-component adsorption equilibrium isotherms parameters (Langmuir isotherm) are presented in Table 3.

Since oxygen and argon capacities are very similar, feed was considered to be 78% of nitrogen and 22% of a pseudo-binary mixture of oxygen and argon.

The operating conditions, the physical characteristics and valve coefficients considered in the simulations are given in Table 4.

The feed flow rate given by the compressor is (Santos et al., 2004):

$$u_{\text{in}} p_{\text{T}} = \frac{10^{-3} p^0 T}{60 \varepsilon A T^0 u_{\text{ref}} p_{\text{ref}}} [0.0731 (p_{\text{T}} p_{\text{ref}})^3 - 0.288 (p_{\text{T}} p_{\text{ref}})^2 - 6.517 p_{\text{T}} p_{\text{ref}} + 91.370] \tag{70}$$

In Table 5 we present the effect of mesh refinement in the simulation results (oxygen purity and recovery) for different production flow rates using QUICK scheme. As we can see, for low product flow rates, oxygen purity is higher than 1, simultaneously the concentration profile inside the column present some unphysical oscillations, which do not disappear with mesh refinement. For higher product flow rates the concentration profile inside the column tends to be smoother and unphysical oscillations tend to disappear. These results give us an indication of the number of

Table 4
Operating conditions, physical characteristics and valve coefficients of the PSA unit (Santos et al., 2004)

T (°C)	p_{T}^{H} (MPa)	p_{T}^{L} (MPa)	$t_{\text{pres/prod}}$ (s)	K_{v}^{P}	K_{v}^{ST}	K_{v}^{V}	L (cm)	D (cm)	L^{ST} (cm)
37	0.3	0.1	9.0	0.0394	0.15	0.55	29.5	8.0	12.5

Table 5
Effect of mesh refinement in simulation results (oxygen purity and recovery) for different production flow rates using QUICK scheme

n	1 dm^3_{PTN}/min		3 dm^3_{PTN}/min		5 dm^3_{PTN}/min	
	Rec	Pur	Rec	Pur	Rec	Pur
4	0.070	1.213	0.179	1.045	0.247	0.844
8	0.060	1.041	0.178	1.039	0.245	0.837
16	0.057	0.995	0.172	1.006	0.228	0.779
32	0.057	1.000	0.171	1.001	0.222	0.757
64	0.057	1.000	0.171	1.000	0.222	0.756
128	0.057	1.000	0.171	1.000	0.222	0.756

volumes that are required to accurately simulate this separation unit. A number of 32 volumes are apparently acceptable.

In Fig. 9 the error of the solution, ϕ, is presented as a function of the number of discretization volumes for two different schemes: QUICK and SMART for a product flow rate of 1 dm^3_{PTN}/min. In this figure, ϕ is defined as it follows:

$$\phi_i = \frac{|X_i - X_i^{ref}|}{|X_i^{QUICK} - X_i^{ref}|} \quad (71)$$

where X_i^{ref} is the reference oxygen purity (or recovery) in the outlet stream, X_i the oxygen purity (or recovery) using i discretization volumes, X_i^{QUICK} the oxygen purity (or recovery) using four discretization volumes and QUICK scheme. As we can see, the error in the simulation results using QUICK scheme tends, with mesh refinement, to an asymptotic error which is not obvious from the analysis of Table 2. Note that this is due to the unbounded properties of QUICK scheme.

In Fig. 10 we present the comparison between experimental results, simulation results using SMART scheme, and the simulation results by Santos et al. (2004). We can observe a good agreement between experimental and simulation results.

Our strategy was also used to analyse the influence of the discretization scheme and mesh refinement in the results of numerical optimization of such a unit using six decision variables: L/L^{ST} (assuming that the area of storage tank and columns

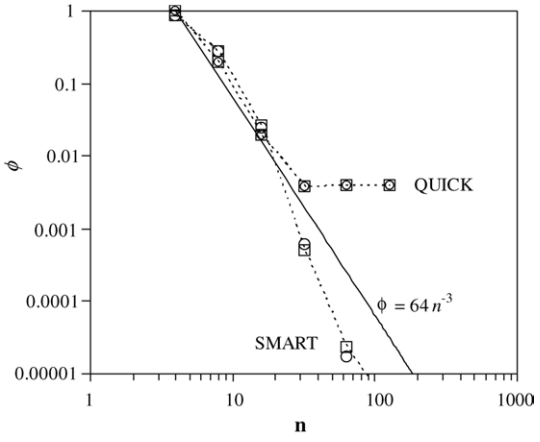

Fig. 9. Effect of mesh refinement on oxygen purity and recovery (cyclic steady-state): (□) purity and (○) recovery, using QUICK and SMART schemes.

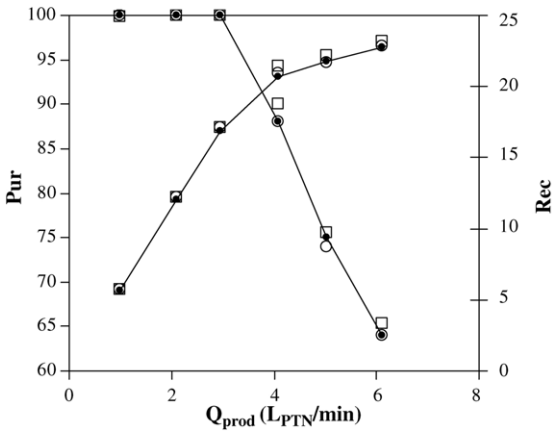

Fig. 10. Purity and recovery as a function of production flow rate: (□) SMART scheme, (○) Santos et al. (2004) values and (●) experimental.

are the same) $\theta_{pres/prod}$ C_v^F, C_v^{ST}, C_v^P and C_v^V. In Table 6 we present the optimization results for a temperature of 20 °C, for details see Santos et al. (2004). A ϕ value of 110 was considered and a restriction of oxygen + argon purity of 0.99 was imposed in the optimization. The time cycle is the variable that is more affected with mesh refinement. The maximum recovery obtained increases with mesh refinement as expected.

As a conclusion on this topic, we should remark that it should be avoid the use of unbounded schemes in the solution of cyclic adsorption processes, namely when the problem involves sharp moving fronts, since with this schemes the error in the problem solution decreases with mesh refinement very slowly (in the case of QUICK scheme the third-order accuracy is completely lost).

7.3. Simulated moving bed

Simulated moving bed (SMB) technology (Boughton, 1961) is an emerging technology for the separation of life science products, such as pharmaceuticals, proteins, enzymes, food and fine chemicals, where standard thermal unit operations like distillation are not suitable. It provides a powerful tool for the separation of multicomponent mixtures in which the components have different adsorption affinities, especially when they show separation factors near one and when high resolutions, yields and purities are required.

Originally developed as an industrial process by Broughton (1984) for the large-scale separation of C8 aromatic hydro-

Table 6
Effect of mesh refinement in optimization results using SMART scheme

n	L/L^{ST}	$\theta_{pres/prod}$	C_v^F	C_v^{ST}	C_v^P	C_v^V	Rec
4	2.06	0.73	155	73.4	9.0	229	0.252
8	2.09	0.90	155	73.4	8.9	229	0.288
16	2.10	1.06	155	73.4	8.9	229	0.317
32	2.02	1.10	155	73.4	8.8	229	0.324
64	2.10	1.11	155	73.4	8.9	229	0.324
128	2.10	1.11	155	73.4	8.9	229	0.324

carbons and sugars, SMB is now considered as the process of choice for the separation of optical isomers.

In the case of petrochemicals (C8 aromatics) and food (C6 sugars) industries the separation factors are very large, the column efficiency does not need to be high and there are solid phases available on which the adsorption equilibrium isotherms are almost linear within the entire useful range of concentrations. The situation is, however, quite different for the enantiomeric separations considered in the pharmaceutical industry. In most cases, the separation factor is low and the isotherms are not usually linear.

The type of isotherm influences substantially the structure of the resulting mathematical problem. Processes with linear adsorption isotherms can be modeled and simulated much more easily than those with non-linear isotherms (Zhong, Yun, Khattabi, & Guiochon, 1997).

Different numerical methods have been applied to the simulated moving bed technology using the method of lines: successive stages method (Charton & Nicoud, 1995; Ludemann-Hombourger et al., 2000), finite differences (Kaczmarski & Antos, 1996), orthogonal collocation (Wang & Ching, 2004) and orthogonal collocation in finite elements (Leão & Rodrigues, 2004; Minceva, Pais, & Rodrigues, 2003).

Recently, Leão and Rodrigues (2004) presented a comparative study of different numerical strategies. For the solution of dynamic models they used two different strategies: the public domain package PDECOL, that uses the method of lines and a B-splines finite element collocation procedure and the DASSL public domain stiff solver (based on backward differentiation formulae) for time integration and orthogonal collocation in finite elements for spatial discretization (Hermite polynomials). For the steady-state models they use the COLDAE and COLNEW public domain solvers.

7.3.1. Mass exchange rate

In simulated moving bed the mass exchange rate between the particle and its surroundings is given by the following expression:

$$N_i = \frac{1-\varepsilon_b}{\varepsilon_b}\frac{\partial \bar{q}_i}{\partial t} \tag{72}$$

where ε_b is the bed void fraction and $\bar{q}_i$ the average molar concentration in the adsorbed phase.

7.3.2. Intra-particle mass transfer

Different approximations can be considered for describing the intra-particle mass transfer. In this work we use the linear driving force approximation (Glueckauf, 1955), as in the case of cyclic adsorption processes:

$$\frac{d\bar{q}_i}{d\theta} = k_i(q_{i,s} - \bar{q}_i) \tag{73}$$

where k_i is the LDF coefficient, $q_{i,s}$ the molar concentration in the particle surface (adsorbed phase) that is related with molar concentration in the inter-particle fluid phase through the adsorption equilibrium isotherm: $q_{i,s} = f(c_i)$.

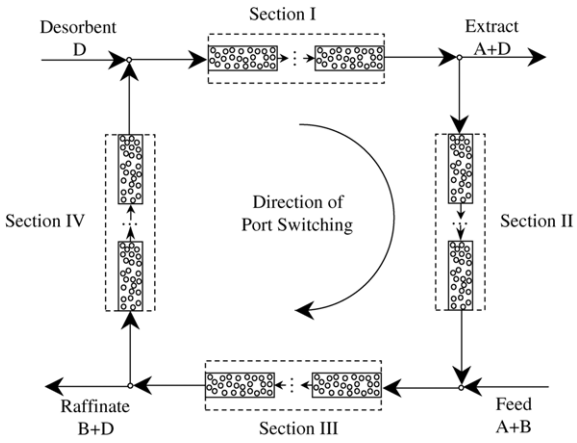

Fig. 11. Representation of simulated moving bed process.

7.3.3. Results and discussion

Simulated moving bed uses a variable number of columns, distributed by four different sections as illustrated in Fig. 11. In-between these sections there are four nodes: extract outlet, feed inlet, raffinate outlet and desorbent inlet.

The mass balance at the nodes are:

- Desorbent node:

$$Q_{IV} + Q_D = Q_I; \qquad c_{i,IV}^{out} Q_{IV} = c_{i,I}^{in} Q_I, \quad i = A, B$$

- Extract node:

$$Q_{II} = Q_I - Q_E$$

- Feed node:

$$Q_{II} + Q_F = Q_{III}; \qquad c_{i,II}^{out} Q_{II} + c_{i,in} Q_{in} = c_{i,III}^{in} Q_{III}, \quad i = A, B$$

- Raffinate node:

$$Q_{III} - Q_R = Q_{IV}$$

Here Q_j is the liquid flowrate throught section j and $c_{i,in}$ the feed concentration of component i. The boundary conditions applied to each of n column are the basic Danckwerts boundary conditions. In this work, as test case, we consider the glucose(A)/fructose(B) separation with a 12-column configuration (3, 3, 3, 3) considering linear isotherms as described by Leão and Rodrigues (2004). The operating conditions and model parameters used in the simulations are presented in Table 7.

In Fig. 12 we present the solution of the model equations using four control volumes in each section (solution of $32 = 4 \times 4 \times 2$ algebraic equations) using QUICK (a) and SMART (b) schemes. The solution using the unbounded QUICK scheme presents an unphysical overshoot in fructose concentration in section II. The bounded SMART scheme does not present

Table 7
Model parameters and operating conditions

Model parameters	Operating conditions
Peclet number: $Pe_j = u_j L/D_{ax} = 2000\gamma_j$	Feed concentration: $c_i^F = 30$ g/l
Solid/fluid ratio: $(1-\varepsilon_b)/\varepsilon_b = 1.5$	
Number of transfer units: $k_i L/u_{ref} = 31.5$	
Ratio between fluid and solid velocities: $\gamma_I = 1.0149$, $\gamma_{II} = 0.6122$, $\gamma_{III} = 0.7039$, $\gamma_{IV} = 0.4252$	
Isotherm parameters: $q_A = 0.3401 c_A$, $q_B = 0.5634 c_B$	

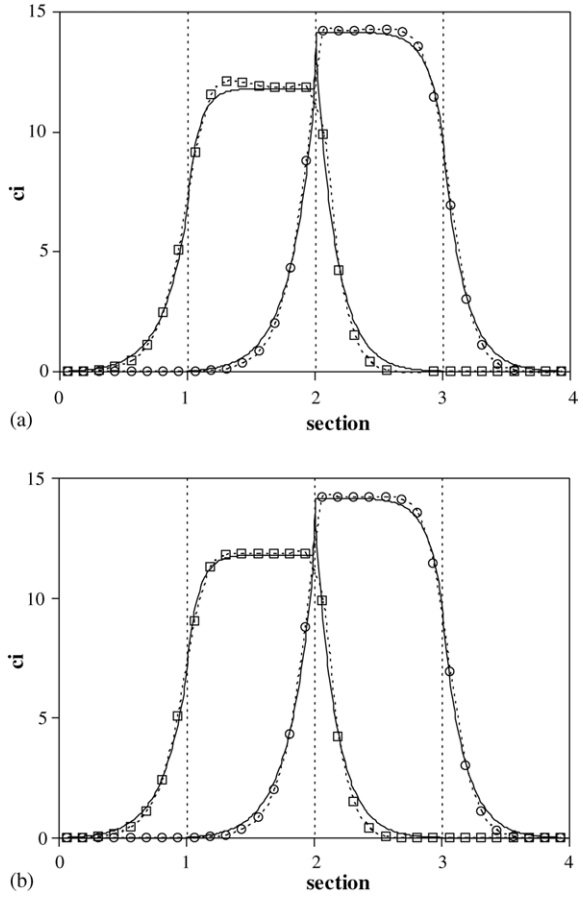

Fig. 12. Solution of simulated moving bed model using parameters from Table 3, (□) frutose, (◯) glucose concentration; (a) solution using QUICK scheme and (b) solution using SMART scheme; (—) reference solution.

this problem. What is remarkable from the analysis of this figure is that using only four control volumes the solution is practically identical to the reference solution (obtained using a very refined mesh).

In Table 8 we present the effect of mesh refinement in simulation results using SMART scheme. We can see that eight control volumes in each section (64 algebraic equations) are in this case sufficient to obtain a good solution. Using finite volume method the conservation of mass is always ensured. Leão and Rodrigues (2004) report errors in the mass balance of 3% for glucose and 4% for fructose using finite elements collocation (Hermite polynomials) and 0.3% for glucose and 0.4% for fructose using COLNEW and COLDAE public domain solvers. The calculation time for a mesh of 16 control volumes is inferior to one second in a 1.5 GHz Intel Pentium IV® personal computer.

In Fig. 12 is presented the error of the solution, ϕ as a function of the number of discretization volumes for three different schemes: Upwind (UDS), MINMOD and SMART. In this figure, ϕ is defined as it follows:

$$\phi_i = \frac{|c_i - c_i^{ref}|}{|c_i^{UDS} - c_i^{ref}|} \tag{74}$$

where c_i^{ref} is the reference fructose (or glucose) concentration, c_i the fructose (or glucose) concentration using i discretization volume and c_i^{UDS} the fructose (or glucose) concentration using four volumes and UDS scheme.

One more time we can see that SMART scheme has a convergence order of 3, MINMOD scheme a convergence order of 2 and upwind has only first-order convergence (Fig. 13).

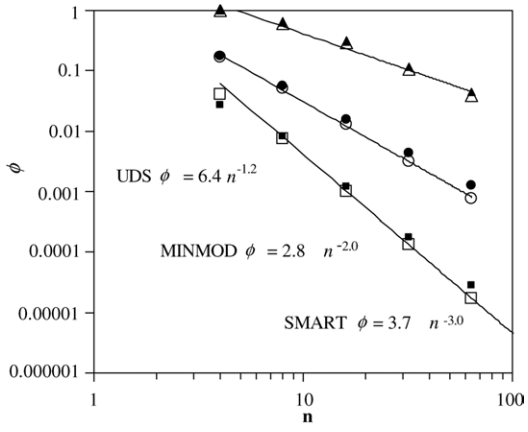

Fig. 13. Effect of mesh refinement: open symbols—fructose concentration (extract) and close symbols—glucose concentration (raffinate).

Table 8
Effect of mesh refinement, SMART scheme

n	t (s)	Glucose concentration				Fructose concentration			
		Eluent	Extract	Feed	Raffinate	Eluent	Extract	Feed	Raffinate
4	0.1	0.030	0.061	14.00	9.78	0.014	6.72	13.81	0.158
8	0.2	0.000	0.003	14.19	9.87	0.001	6.83	14.19	0.000
16	0.7	0.002	0.015	14.17	9.85	0.005	6.82	14.18	0.019
32	3.3	0.003	0.017	14.17	9.85	0.005	6.82	14.18	0.022
64	14.6	0.003	0.017	14.17	9.85	0.005	6.82	14.18	0.023

8. Conclusions

In this work we describe the application of finite volume method for the solution of separation processes involving adsorption, absorption and permeation. The algorithm presented enforces both local and global flux conservation in space and time. The convection terms can be discretized using high-resolution schemes, ensuring boundedness. We present numerical results for three different separation processes: membrane permeation, pressure swing adsorption and simulated moving bed, to highlight the flexibility, efficiency and robustness of the proposed formulation.

We have demonstrated the virtues of using an algorithm that ensures local and global flux conservation in space and time. Comparatively with other strategies we obtain better solutions with less number of discretization points, hence, using less computation time and memory requirements.

In the case of membrane permeation we have compared our results with the successive stages method proposed by Coker et al. (1998). We have seen that successive stages method has only first-order of convergence and so, when the stage cut is very high (>90%), it requires at lest 1000 discretization points to obtain the problem solution.

In the case of cyclic adsorption processes we simulated a small pressure swing adsorption unit for oxygen production described by Santos et al. (2004), for understanding the convergence of different discretization schemes. The use of 32 volumes was found to be sufficient for assuring a good accuracy of the results. The simulation results were verified to be in very good agreement with the experimental results presented by Santos et al. (2004). We have also used our package to optimize the unit (select the best cycle time and orifices pressure drop) and to study the influence of the number of discretization volumes in the optimization variables and results. The optimal recovery increases with mesh refinement and the pressurization/ production step duration is highly influenced by the number of volumes.

In the case of simulated moving bed, we have considered the glucose(A)/fructose(B) separation as described by Leão and Rodrigues (2004). In this case we concluded that 8 control volumes in each section (solution of 64 algebraic equations) are sufficient to obtain an accurate solution. We have seen that the conservation of mass is always ensured using finite volume method. Note that, Leão and Rodrigues (2004) report errors in the mass balance of 3% for glucose and 4% for fructose using finite elements collocation (Hermite polynomials) and 0.3% for glucose and 0.4% for fructose using COLNEW and COLDAE public domain solvers.

From the simulation of three different separation processes we found that our numerical strategy, based on finite volume method using high-resolution schemes, permits to obtain accurate solutions, assuring both local and global flux conservation and without unphysical oscillations.

Acknowledgements

The work of Paulo Cruz and João Carlos Santos was supported by FCT, grants POSI SFRH/BPD/13539/2003 and SFRH/BD/6817/2001, respectively. The research was also supported by funds from FCT project POCTI/EQU/38067/2001 and Growth GRDI-2001-40257.

References

Alves, M. A., Oliveira, P. J., & Pinho, F. T. (2003). A convergent and universally bounded interpolation scheme for the treatment of advection. *International Journal for Numerical Methods in Fluids*, *41*, 47.

Arvind, R., Farooq, S., & Ruthven, D. M. (2002). Analysis of a piston PSA process for air separation. *Chemical Engineering Science*, *57*, 419.

Bird, R. B., Stewart, W. E., & Lightfoot, E. N. (1960). *Transport phenomena*. New York: Wiley.

Boucif, N., Majumdar, S., & Sirkar, K. K. (1984). Series solutions for a gas permeator with countercurrent and cocurrent flow. *Industrial and Engineering Chemistry Fundamentals*, *23*, 470.

Boughton, D. B. (1961). *Continuous sorption process employing fixed bed of sorbent and moving inlets and outlets*. U.S. Patent 2 985 589.

Broughton, D. B. (1984). Production-scale adsorptive separations of liquid-mixtures by simulated moving-bed technology. *Separation Science and Technology*, *19*, 723.

Byrne, G. D., Hindmarsh, A. C., Jackson, K. R., & Brown, H. G. (1977). Comparison of 2 ODE codes—gear and episode. *Computers and Chemical Engineering*, *1*, 133.

Cen, P., & Yang, R. T. (1985). Separation of a 5-component gas-mixture by pressure swing adsorption. *Separation Science and Technology*, *20*, 725.

Chang, D., Min, J., Oh, S., & Moon, K. (1998). Perturbation solution of hollow-fiber membrane module for pure gas permeation. *Journal of Membrane Science*, *143*, 53.

Charton, F., & Nicoud, R. M. (1995). Complete design of a simulated moving-bed. *Journal of Chromatography A*, *702*, 97.

Chen, Y. S., Li, K., & Teo, W. K. (1995). Performance of co counter-current and counter co-current flow patterns in an internally staged permeator for gas separation. *Chemical Engineering Research and Design*, *73*, 567.

Cheng, H. C., & Hill, F. B. (1985). Separation of helium–methane mixtures by pressure swing adsorption. *AIChE Journal*, *31*, 95.

Chou, C. T., & Huang, W. C. (1994). Simulation of a 4-bed pressure swing adsorption process for oxygen enrichment. *Industrial and Engineering Chemistry Research*, *33*, 1250.

Coker, D. T., Allen, T., Freeman, B. D., & Fleming, G. K. (1999). Nonisothermal model for gas separation hollow-fiber membranes. *AIChE Journal*, *45*, 1451.

Coker, D. T., Freeman, B. D., & Fleming, G. K. (1998). Modeling multicomponent gas separation using hollow-fiber membrane contactors. *AIChE Journal*, *44*, 1289.

Courant, R., Isaacson, E., & Rees, M. (1952). On the solution of nonlinear hyperbolic differential equations by finite differences. *Communications on Pure and Applied Mathematics*, *5*, 243.

Cruz, P., Santos, J. C., Magalhães, F. D., & Mendes, A. (2003). Cyclic adsorption separation processes: Analysis strategy and optimization procedure. *Chemical Engineering Science*, *58*, 3143.

Da Silva, F. A., Silva, J. A., & Rodrigues, A. E. (1999). A general package for the simulation of cyclic adsorption processes. *Adsorption*, *5*, 229.

Danckwerts, P. V. (1953). Continuous flow systems—distribution of residence times. *Chemical Engineering Science*, *2*, 1.

Darwish, M. S., & Moukalled, F. H. (1994). Normalized variable and space formulation methodology for high-resolution schemes. *Numerical Heat Transfer Part B: Fundamentals*, *26*, 79.

Fehlberg, E. (1968). Classical fifth, sixth, seventh, and eighth order Runge–Kutta formulas with stepsize control, *NASA Technical Report 287*. Marshall: George C. Marshall Space Flight Center.

Finlayson, B. (1992). *Numerical methods for problems with moving fronts*. Seattle, Washington, USA: Ravenna Park Publishing Inc.

Freitas, C. J. (1994). Policy statement on the control of numerical accuracy—response. *Journal of Fluids Engineering—Transactions of the ASME, 116*, 198.

Gaskell, P. H., & Lau, A. K. C. (1988). Curvature-compensated convective-transport—smart, a new boundedness-preserving transport algorithm. *International Journal for Numerical Methods in Fluids*, *8*, 617.

Gear, G. W. (1971). *Numerical initial-value problems in ordinary differential equations*. Englewood Cliffs: Prentice-Hall.

Glueckauf, E. (1955). Theory of chromatography 10. Formulae for diffusion into spheres and their application to chromatography. *Transactions of the Faraday Society*, *51*, 1540.

Harten, A. (1983). High-resolution schemes for hyperbolic conservation-laws. *Journal of Computational Physics*, *49*, 357.

Harten, A. (1996). Multiresolution representation of data: A general framework. *Siam J Numer Anal*, *33*, 1205.

Harten, A., Engquist, B., Osher, S., & Chakravarthy, S. R. (1987). Uniformly high-order accurate essentially nonoscillatory schemes, Part 3. *Journal of Computational Physics*, *71*, 231.

Hindmarsh, A. C. (1974). Gear: Ordinary differential equation system solver, *Technical Report UICD-30001*, Rev. 3. Lawrence, California: Lawrence Livermore Laboratories.

Kaczmarski, K., & Antos, D. (1996). Fast finite difference method for solving multicomponent adsorption-chromatography models. *Computers and Chemical Engineering*, *20*, 1271.

Kaldis, S. P., Kapantaidakis, G. C., Papadopoulos, T. I., & Sakellaropoulos, G. P. (1998). Simulation of binary gas separation in hollow fiber asymmetric membranes by orthogonal collocation. *Journal of Membrane Science*, *142*, 43.

Knaebel, K. S., & Hill, F. B. (1985). Pressure swing adsorption—development of an equilibrium-theory for gas separations. *Chemical Engineering Science*, *40*, 2351.

Ko, D., & Moon, I. (2000). Optimization of start-up operating condition in RPSA. *Separation and Purification Technology*, *21*, 17.

Kovvali, A. S., Vemury, S., Krovvidi, K. R., & Khan, A. A. (1992). Models and analyses of membrane gas permeators. *Journal of Membrane Science*, *73*, 1.

Leão, C. P., & Rodrigues, A. E. (2004). Transient and steady-state models for simulated moving bed processes: Numerical solutions. *Computers and Chemical Engineering*, *28*, 1725.

Leonard, B. P. (1979). Stable and accurate convective modeling procedure based on quadratic upstream interpolation. *Computer Methods in Applied Mechanics and Engineering*, *19*, 59.

Leonard, B. P. (1987). Locally modified quick scheme for highly convective 2-D and 3-D flows. In C. Taylor & K. Morgan (Eds.), *Numerical methods in laminar and turbulent flow: Vol. 5* (p. 35). Swansea, UK: Pineridge Press.

Leonard, B. P. (1995). Order of accuracy of quick and related convection-diffusion schemes. *Applied Mathematical Modelling*, *19*, 640.

Liaw, C. H., Wang, J. S. P., Greenkorn, R. A., & Chao, K. C. (1979). Kinetics of fixed-bed adsorption—new solution. *AIChE Journal*, *25*, 376.

Ludemann-Hombourger, O., Nicoud, R. M., & Bailly, M. (2000). The "Varicol" process: A new multicolumn continuous chromatographic process. *Separation Science and Technology*, *35*, 1829.

Mendes, A., Magalhães, F., & Costa, C. (2003). New trends on membrane science. In J. Fraissard & C. W. Conner (Eds.), *Fluid transport in nanoporous materials*. Kluwer Academic Publishers.

Minceva, M., Pais, L. S., & Rodrigues, A. E. (2003). Cyclic steady state of simulated moving bed processes for enantiomers separation. *Chemical Engineering and Processing*, *42*, 93.

Nilchan, S., & Pantelides, C. C. (1998). On the optimisation of periodic adsorption processes. *Adsorption*, *4*, 113.

Pan, C. Y. (1983). Gas separation by permeators with high-flux asymmetric membranes. *AIChE Journal*, *29*, 545.

Pettersen, T., & Lien, K. M. (1994). A new robust design-model for gas separating membrane modules, based on analogy with countercurrent heat-exchangers. *Computers and Chemical Engineering*, *18*, 427.

Petzold, L. (1983). Automatic selection of methods for solving stiff and nonstiff systems of ordinary differential-equations. *SIAM Journal on Scientific and Statistical Computing*, *4*, 136.

Purnomo, I. S. K., & Alpay, E. (2000). Membrane column optimisation for the bulk separation of air. *Chemical Engineering Science*, *55*, 3599.

Raghavan, N. S., Hassan, M. M., & Ruthven, D. M. (1985). Numerical-simulation of a PSA system. 1. Isothermal trace component system with linear equilibrium and finite mass-transfer resistance. *AIChE Journal*, *31*, 385.

Raghavan, N. S., & Ruthven, D. M. (1985). Pressure swing adsorption. 3. Numerical-simulation of a kinetically controlled bulk gas separation. *AIChE Journal*, *31*, 2017.

Santos, J. C., Portugal, A. F., Magalhães, F. D., & Mendes, A. (2004). Simulation and optimization of small oxygen pressure swing adsorption units. *Industrial and Engineering Chemistry Research*, *43*, 8328.

Shendalm, L. H., & Mitchell, J. E. (1972). Study of heatless adsorption in model system CO_2 in He, Part 1. *Chemical Engineering Science*, *27*, 1449.

Sherman, J. D. (1999). Synthetic zeolites and other microporous oxide molecular sieves. *Proceedings of the National Academy of Sciences of the United States of America*, *96*, 3471.

Shu, C. W. (1997). Essentially nonoscillatory (ENO) and weighted essentially nonoscillatory (WENO) schemes for hyperbolic conservation laws. In B. Cockburn, C. Johnson, C. W. Shu, E. Tadmor, & A. Quarteroni (Eds.), *Advanced numerical approximation of nonlinear hyperbolic equations: Lecture notes in Mathematics: Vol. 1697* (p. 32). Berlin: Springer-Verlag.

Shu, C. W., & Osher, S. (1988). Efficient implementation of essentially non-oscillatory shock-capturing schemes. *Journal of Computational Physics*, *77*, 439.

Shu, C. W., & Osher, S. (1989). Efficient implementation of essentially non-oscillatory shock-capturing schemes, Part 2. *Journal of Computational Physics*, *83*, 32.

Shyy, W. (1985). A study of finite-difference approximations to steady-state, convection-dominated flow problems. *Journal of Computational Physics*, *57*, 415.

Smith, S. W., Hall, C. K., Freeman, B. D., & Rautenbach, R. (1996). Corrections for analytical gas-permeation models for separation of binary gas mixtures using membrane modules. *Journal of Membrane Science*, *118*, 289.

Teague, K. G., & Edgar, T. F. (1999). Predictive dynamic model of a small pressure swing adsorption air separation unit. *Industrial and Engineering Chemistry Research*, *38*, 3761.

Tessendorf, S., Gani, R., & Michelsen, M. L. (1999). Modeling, simulation and optimization of membrane-based gas separation systems. *Chemical Engineering Science*, *54*, 943.

Thundyil, M. J., & Koros, W. J. (1997). Mathematical modeling of gas separation permeators—for radial crossflow, countercurrent, and cocurrent hollow fiber membrane modules. *Journal of Membrane Science*, *125*, 275.

Wang, X., & Ching, C. B. (2004). Chiral separation and modeling of the three-chiral-center [beta]-blocker drug nadolol by simulated moving bed chromatography. *Journal of Chromatography A*, *1035*, 167.

Weller, S., & Steiner, W. A. (1950). Engineering aspects of separation of gases—fractional permeation through membranes. *Chemical Engineering Progress*, *46*, 585.

Yang, J. Y., & Lee, C. H. (1998). Adsorption dynamics of a layered bed PSA for H_2 recovery from coke oven gas. *AIChE Journal*, *44*, 1325.

Zhang, Z. Y., Hidajat, K., Ray, A. K., & Morbidelli, M. (2002). Multiobjective optimization of smb and varicol process for chiral separation. *AIChE Journal*, *48*, 2800.

Zhong, G., Yun, T., Khattabi, Y., & Guiochon, G. (1997). Simulated moving bed chromatography under linear conditions. *Chromatographia*, *45*, 109.